SS_Wave_Excitation_Fitting_Report_draft

Theory and User Manual

Alan Wright
Jason Jonkman
Amy Robertson
Greg Hayman

Draft: 02/3/2019

Contents

1. Introduction

Placing wind turbines on offshore floating platforms poses many challenges to a low-cost system design. These dynamically active systems are subject to stochastic wind and wave inputs which drive fatigue loads. The effects of these disturbances must be mitigated by the wind turbine controller to reduce critical loads and realize lower cost of energy.

OpenFAST, developed by the National Renewable Energy Laboratory (NREL), is a coupled analysis tool for modeling floating offshore wind turbines [1]. HydroDyn, the hydrodynamic module included in OpenFAST, is currently based on a hybrid combination of strip theory and potential flow, including first- and second-order effects (this report; however, only addresses linear wave-excitation from potential flow) [2]. The module employs the general form of the Cummins equation, including the effect of hydrostatics, wave excitation, and wave radiation [3]. The wave radiation and excitation forces are usually calculated using inverse Fourier Transforms or convolution integrals which are not well suited to the simplified models needed for rapid design optimization and advanced controller design. Linear state-space models are better suited for these goals.

The goal for advanced controller design is develop linear state-space models for the full turbine platform system in OpenFAST. Figure 1 shows a system diagram of the overall floating system, with inputs from wave excitation and wave radiation forces (acting on the platform), as well as wind and controller inputs (acting on the turbine). To obtain an overall state-space model of this entire system, the models for the wave excitation and wave radiation forces must be linearized and expressed in state-space form. The state-space models for the wave radiation and wave

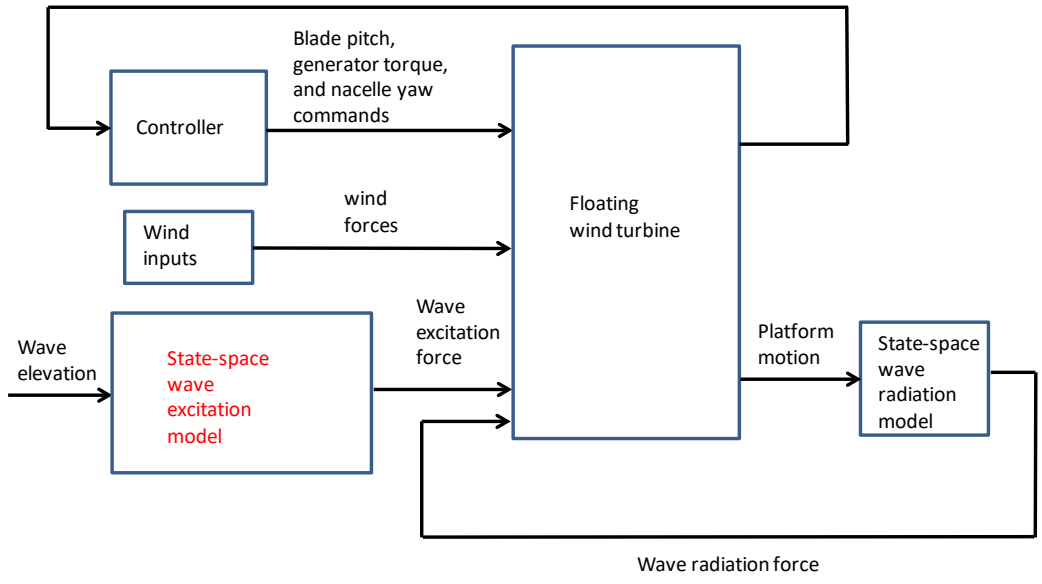

Figure 1. FAST Modules Including the Floating wind turbine with different sub-system components, inputs, and outputs.

excitation forces can then be imbedded in FAST's HydroDyn module and used in the overall linearization approach to obtain a linear state-space model of the full system [4].

The development of a state-space model representing the wave radiation force system has already been described in [5,6]. **The focus of the work in this report is the development of a state-space modeling method for the external wave excitation forces**. The state-space model takes wave elevation as the input and outputs the wave excitation forces acting on the floating platform (the part of the system highlighted in red in Fig. 1). The usual method of calculating these forces is through Inverse Fourier Transform (IFT) calculations, as will be described in Section 2. We want to replace the IFT method of calculating wave forces with the state-space approach. This new model will be imbedded in OpenFAST's HydroDyn module. An issue that must be addressed in formulating a method to generate this wave excitation state-space model is the non-causality of the excitation force system when wave elevation (measured at the platform origin of coordinates) is used as the input to the model [7,8]. We will address this issue in Section 2.

The method of generating a linear state-space model for the wave excitation force system has been programmed as a set of MatLab routines to be described in the Appendix of this report. These routines read frequency-domain wave-excitation loads for a given platform from the output of the panel code Wamit [9]. They then calculate a causal impulse response function (IRF) for the platform. A state-space model representation of the system is then determined from the causal impulse response function, with wave elevation as the input and the wave forces acting on the platform as the output.

This report is organized as follows: Section 2 describes the theory supporting the wave excitation state-space modeling approach. This section also addresses the causality issue. Section 3 describes the approach for fitting a state-space model to the resulting causal IRF. Section 4 describes the assembly of the individual state-space models corresponding to each platform degree of freedom (DOF) into a global state-space model. Section 5 shows a comparison between the wave excitation forces calculated using HydroDyn's IFT method versus the state-space approach. These comparisons are made for two floating platform configurations. Finally, Appendix A is a User's Guide for the MatLab routines that generate these state-space models.

2. Linear Hydrodynamic Theory

2.1. Time-domain Models

The hydrodynamic forces applied to a free-floating body can be described as the combination of terms related to various force contributions. For each DOF i,

$$F_i^{\text{hydrodynamic}} = F_i^{\text{hydrostatic}} + F_i^{\text{radiation}} + F_i^{\text{waves}} \quad (i = 1, 2, \ldots, 6), \tag{1}$$

where $F_i^{\text{hydrodynamic}}$ is the 1st order hydrodynamic loads acting on the platform. The terms on the right hand side of equation [1] describe the hydrostatic restoring ($F^{\text{hydrostatic}}$), wave radiation

($F^{\text{radiation}}$), and wave excitation (F^{waves}) forces. In general, these forces are each represented by a 6x1 vector, with each vector entry i corresponding to a force input for one of six degrees of freedom of platform motion.

Here we focus on the wave excitation force vector F^{waves}. In the frequency domain, the wave excitation force can be expressed [3]:

$$F_i^{\text{waves}}(\omega) = K_{\text{Exctn}_i}(\omega)\varsigma(\omega), \tag{2}$$

where ω is wave frequency, $\varsigma(\omega)$ is the complex wave height spectrum (including random phases), and $K_{\text{Exctn}_i}(\omega)$ is the wave excitation frequency response function (FRF) for the i^{th} force component. For time-domain simulations of floating offshore wind turbines (FOWTs), the spectral wave data is a model input. The force vector F^{waves} (dropping subscript *i* for now) in the time domain must be calculated prior to the turbine-platform simulation in HydrDyn for all six directions. The approach used in HydroDyn is to calculate the Inverse Fourier Transform (IFT) of the frequency response function multiplied by the wave spectrum [3] (then implementing in HydroDyn computes the IFT numerically using a Discrete Fourier Transform (DFT)):

$$F^{\text{waves}}(t) = \frac{1}{2\pi}\int_{-\infty}^{\infty} K_{\text{Exctn}}(\omega)\varsigma(\omega)e^{j\omega t}d\omega. \tag{3}$$

Here, j is the imaginary number $\sqrt{-1}$. Alternatively, the wave excitation force components can be calculated through a convolution integral:

$$F^{\text{waves}}(t) = \int_{-\infty}^{\infty} K_{\text{Exctn}}(t-\tau)\varsigma(\tau)d\tau = K_{\text{Exctn}}(t) * \varsigma(t), \tag{4}$$

where * represents convolution, and $K_{\text{Exctn}}(t) = \frac{1}{2\pi}\int_{-\infty}^{\infty} K_{\text{Exctn}}(\omega)e^{j\omega t}d\omega$. (5)

$K_{\text{Exctn}}(t)$ represents the platform's wave excitation Impulse Response Function (IRF), which is a 6x1 vector with entries corresponding to each DOF. It depends only on platform parameters, water depth, and wave direction.

Neither the convolution integral method or IFT method of wave force calculation are appropriate for determining a linear state-space model of the turbine platform system. To obtain a state-space model, the wave excitation force system must itself be linearized and represented in linear state-space form. The inputs to this state-space model are the wave

elevation time histories $\varsigma(t)$ and the model output is the 6x1 wave excitation force vector $F^{\text{waves}}(t)$ acting on the platform. Figure 2 shows such a state-space model approximation of the convolution integral in equation [4]).

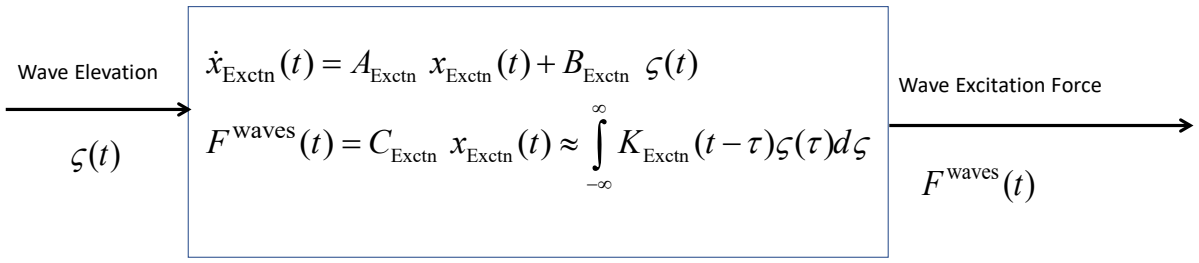

Figure 2. The wave excitation state-space model approximation of the convolution integral.

Before describing the method of generating this state-space model, we must address the causality issue of the wave excitation force system.

2.2. Causality Issue

Fitting a state-space model to the wave excitation system is complicated by the non-causality of this system. The basic issue is that the platform may experience a change in wave forces (at a certain platform reference point) before the wave elevation corresponding to these forces is sensed at this reference point [7,8]. The wave elevation corresponding to the current platform wave forces must be measured a certain distance away from the platform in the wave heading direction. Only then will the measured wave elevations correspond in time to the measured wave forces at the platform reference point. This issue has been studied extensively in [7] where a time shifting method is used to arrive at a causal transfer function (and causal IRF) between wave elevation and wave excitation forces. We follow the method used in [7,8] in this report.

Figure 3 shows an example IRF (blue curve) due to a wave elevation impulse acting at time t=0 seconds (sec.). This IRF corresponds to the platform's pitch DOF. This figure shows that the system is non-causal, since the system's response is nonzero for negative time even though the impulse acts at t=0 sec. The system response for negative time is as large as the response for positive time, so it can't be ignored.

An approximately causal IRF is obtained through time-shifting the original IRF. From Figure 3 it is seen that for all times less than $-t_c$ ($t_c \approx 12$ seconds for this example) the IRF is

approximately zero. A time delay t_c is introduced to shift the original IRF to obtain a causal IRF $K_{\mathrm{Exctn_c}}(t)$:

$$K_{\mathrm{Exctn_c}}(t) = K_{\mathrm{Exctn}}(t - t_c). \tag{6}$$

Figure 3 shows that this time shifted IRF (red) is approximately zero for all negative time.

We can now show that:

$$\begin{aligned} F^{\mathrm{waves}}(t) &= K_{\mathrm{Exctn}}(t) * \varsigma(t) \\ &= K_{\mathrm{Exctn_c}}(t) * \varsigma_c(t) \end{aligned}, \tag{7}$$

where $\varsigma_c(t) = \varsigma(t + t_c)$ is the wave elevation predicted t_c seconds (sec.) into the future (see Appendix B for a proof of equation [7]).

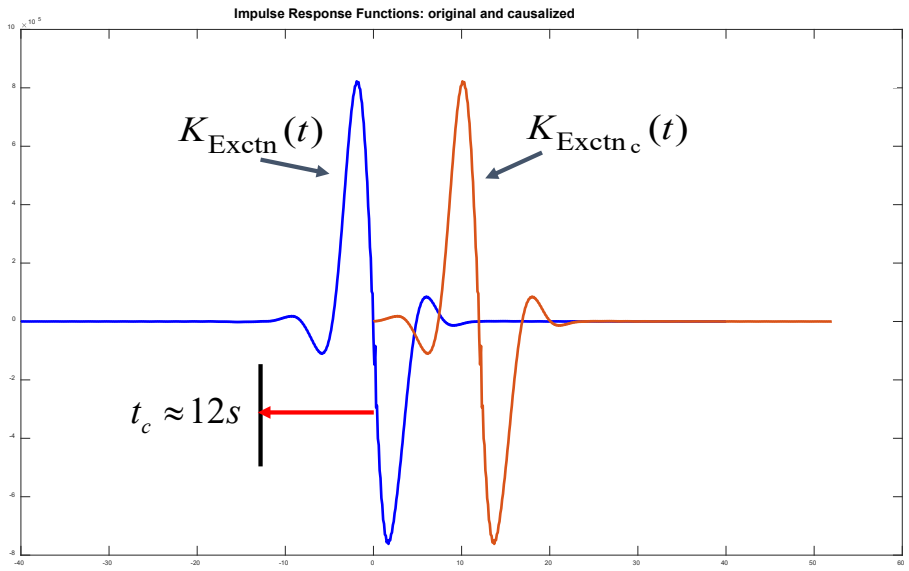

Figure 3. Non-causal and causal Impulse Response Functions for the platform's pitch degree of freedom.

To implement this approach, a wave prediction model must be used to predict the waves t_c sec. into the future. For the overall OpenFAST process, this is not an issue, since the wave elevation data for the wave force calculation is pre-calculated before the simulation, making the wave elevation data at all times available at run-time. The predictions involve a simple

"look-ahead" by t_c seconds into the wave elevation data file to obtain the correct value to input to the state-space model at any time t. Figure 4 depicts this process.

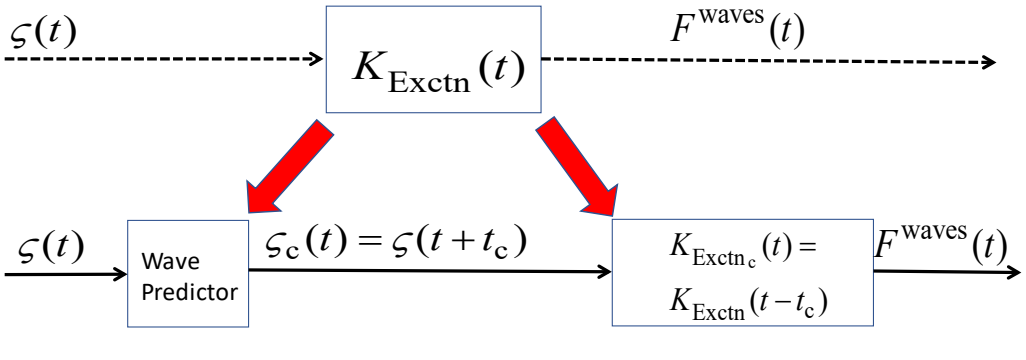

Figure 4. Process for obtaining a causal input-output relationship.

The next step in the process is fitting a state-space model to the causal IRF using system identification.

3. State-space model fitting using system identification

Now, **sys**tem **id**entification (sys id) is used to fit a state-space model approximation to the causal IRF. We use sys id to identify the state-space matrices A_{Exctn}, B_{Exctn} and C_{Exctn} in:

$$\begin{aligned} \dot{x}_{\text{Exctn}}(t) &= A_{\text{Exctn}} x_{\text{Exctn}}(t) + B_{\text{Exctn}} \varsigma_c(t) \\ F^{\text{waves}}(t) &= C_{\text{Exctn}} x_{\text{Exctn}}(t) \end{aligned} \quad . \tag{8}$$

It can be shown that the approximated impulse response function is $K_{\text{Exctn}_c}(t) = C_{\text{Exctn}}\, e^{A_{\text{Exctn}}\, t}\, B_{\text{Exctn}}$, where $e^{A_{\text{Exctn}}\, t}$ is the matrix exponential function [5]. The goal is to determine A_{Exctn}, B_{Exctn}, and C_{Exctn} so that $C_{\text{Exctn}}\, e^{A_{\text{Exctn}}\, t}\, B_{\text{Exctn}}$ approximates $K_{\text{Exctn}_c}(t)$ in terms of some error norm. This is usually done by minimizing a cost function such as:

$$Q = \sum_{k=1}^{m} G(t_k) \left[K_{\text{Exctn}_c}(t_k) - C_{\text{Exctn}} e^{A_{\text{Exctn}}\, t_k} B_{\text{Exctn}} \right]^2 , \tag{9}$$

with $G(t_k)$ a weighting function to be chosen, evaluated at sample times t_k ($k = 1, 2, \ldots, m$).

At least m discrete values of $K_{\mathrm{Exctn_c}}(t_{\mathrm{k}})$ are assumed to be known. Several methods exist for performing this system identification step [5,7,8]. Here we use a state-space realization of the impulse response using Hankel singular value decomposition (SVD) [5] and MatLab's Robust Control Toolbox command **imp2ss** [10]. The state-space model structure is selected so that the infinite frequency limit of the identified model in the frequency domain is zero [10], i.e. $\lim_{\omega\to\infty} G_{\mathrm{i}}(j\omega) = 0.$ Therefore the relative degree is ≥ 1 and the transfer function is strictly proper. This also means that there is no direct feedthrough from the wave elevation input to wave forces (the D_{Exctn} matrix in $F^{\mathrm{waves}}(t) = C_{\mathrm{Exctn}} x_{\mathrm{Exctn}}(t) + D_{\mathrm{Exctn}} \zeta_{\mathrm{c}}(t)$ is the zero matrix).

The function **imp2ss** outputs the matrices of the equivalent system $\bar{A}_{\mathrm{Exctn}}$, $\bar{B}_{\mathrm{Exctn}}$, and $\bar{C}_{\mathrm{Exctn}}$, which need to be scaled according to the time step Δt used in the data of $K_{\mathrm{Exctn_c}}(t)$. So $A_{\mathrm{Exctn}} = \bar{A}_{\mathrm{Exctn}}$, $B_{\mathrm{Exctn}} = \bar{B}_{\mathrm{Exctn}}$, and $C_{\mathrm{Exctn}} = \bar{C}_{\mathrm{Exctn}} \Delta t$.

Despite the option that is built into MatLab's **imp2ss** function, the resulting state-space models have a high order (200-400 states). Computation of the Hankel singular values from these state-space models reveals that only a small number of states have a significant value [5]. A balanced model truncation method is used to arrive at a low-order state-space approximation for the wave excitation force system, using MatLab's **balmr** command [10].

The MatLab script that implements the **balmr** command uses two different methods for assessing the "goodness of fit" of the identified state-space system to the exact system. One is a manual method, in which the user chooses the number of states to keep, based on a visual assessment of the approximated IRFs compared to the original IRF. The second method is an automated procedure, which is implemented using a goodness of fit test.

The goodness of fit test computes the parameter R^2 as:

$$R^2 = 1 - \frac{\sum_l (K_{\mathrm{Exctn_c}} - \hat{K}_{\mathrm{Exctn_c}})}{\sum_l (K_{\mathrm{Exctn_c}} - \bar{K}_{\mathrm{Exctn_c}})}, \tag{10}$$

where $K_{\mathrm{Exctn_c}}$ represents the reference causal IRF, $\hat{K}_{\mathrm{Exctn_c}}$ represents the IRF from the fitted state-space model, and $\bar{K}_{\mathrm{Exctn_c}}$ represents the mean value of the reference IRF. The summations are performed across all time steps using index l. This is a measure of the amount of variability of the function that is captured by the model. The closer that the value R^2 is to one, the better is the quality of the fit [5].

Let's see how the state-space models for each platform DOF are assembled into a global state-space model.

4. Overall State-Space Matrix Assembly

Using the above described methods, a set of state-space matrices is computed, one set for each platform DOF. These individual state-space matrices are then assembled into a global state-space system that contains the sub-matrices for each platform DOF.

For each DOF i the individual state-space equations are:

$$\begin{aligned}\dot{x}_{\mathrm{Exctn_i}}(t) &= A_{\mathrm{Exctn_i}} x_{\mathrm{Exctn_i}}(t) + B_{\mathrm{Exctn_i}} \varsigma_{\mathrm{c}}(t) \\ F_i^{\mathrm{waves}}(t) &= C_{\mathrm{Exctn_i}} x_{\mathrm{Exctn_i}}(t)\end{aligned} \tag{11}$$

The global state-space matrices are assembled as:

$$A_{\mathrm{Exctn}} = \begin{bmatrix} A_{\mathrm{Exctn_1}}{}^{m_1 \, x \, m_1} & 0^{m_1 \, x \, m_2} & 0^{m_1 \, x \, m_3} & 0^{m_1 \, x \, m_4} & 0^{m_1 \, x \, m_5} & 0^{m_1 \, x \, m_6} \\ 0^{m_2 \, x \, m_1} & A_{\mathrm{Exctn_2}}{}^{m_2 \, x \, m_2} & 0^{m_2 \, x \, m_3} & 0^{m_2 \, x \, m_4} & 0^{m_2 \, x \, m_5} & 0^{m_2 \, x \, m_6} \\ 0^{m_3 \, x \, m_1} & 0^{m_3 \, x \, m_2} & A_{\mathrm{Exctn_3}}{}^{m_3 \, x \, m_3} & 0^{m_3 \, x \, m_4} & 0^{m_3 \, x \, m_5} & 0^{m_3 \, x \, m_6} \\ 0^{m_4 \, x \, m_1} & 0^{m_4 \, x \, m_2} & 0^{m_4 \, x \, m_3} & A_{\mathrm{Exctn_4}}{}^{m_4 \, x \, m_4} & 0^{m_4 \, x \, m_5} & 0^{m_4 \, x \, m_6} \\ 0^{m_5 \, x \, m_1} & 0^{m_5 \, x \, m_2} & 0^{m_5 \, x \, m_3} & 0^{m_5 \, x \, m_4} & A_{\mathrm{Exctn_5}}{}^{m_5 \, x \, m_5} & 0^{m_5 \, x \, m_6} \\ 0^{m_6 \, x \, m_1} & 0^{m_6 \, x \, m_2} & 0^{m_6 \, x \, m_3} & 0^{m_6 \, x \, m_4} & 0^{m_6 \, x \, m_5} & A_{\mathrm{Exctn_6}}{}^{m_6 \, x \, m_6} \end{bmatrix},$$

$$B_{\mathrm{Exctn}} = \begin{bmatrix} B_{\mathrm{Exctn_1}}{}^{m_1 \, x \, 1} \\ B_{\mathrm{Exctn_2}}{}^{m_2 \, x \, 1} \\ B_{\mathrm{Exctn_3}}{}^{m_3 \, x \, 1} \\ B_{\mathrm{Exctn_4}}{}^{m_4 \, x \, 1} \\ B_{\mathrm{Exctn_5}}{}^{m_5 \, x \, 1} \\ B_{\mathrm{Exctn_6}}{}^{m_6 \, x \, 1} \end{bmatrix},$$

$$C_{\mathrm{Exctn}} = \begin{bmatrix} C_{\mathrm{Exctn_1}}{}^{1 \, x \, m_1} & 0^{1 \, x \, m_2} & 0^{1 \, x \, m_3} & 0^{1 \, x \, m_4} & 0^{1 \, x \, m_5} & 0^{1 \, x \, m_6} \\ 0^{1 \, x \, m_1} & C_{\mathrm{Exctn_2}}{}^{1 \, x \, m_2} & 0^{1 \, x \, m_3} & 0^{1 \, x \, m_4} & 0^{1 \, x \, m_5} & 0^{1 \, x \, m_6} \\ 0^{1 \, x \, m_1} & 0^{1 \, x \, m_2} & C_{\mathrm{Exctn_3}}{}^{1 \, x \, m_3} & 0^{1 \, x \, m_4} & 0^{1 \, x \, m_5} & 0^{1 \, x \, m_6} \\ 0^{1 \, x \, m_1} & 0^{1 \, x \, m_2} & 0^{1 \, x \, m_3} & C_{\mathrm{Exctn_4}}{}^{1 \, x \, m_4} & 0^{1 \, x \, m_5} & 0^{1 \, x \, m_6} \\ 0^{1 \, x \, m_1} & 0^{1 \, x \, m_2} & 0^{1 \, x \, m_3} & 0^{1 \, x \, m_4} & C_{\mathrm{Exctn_5}}{}^{1 \, x \, m_5} & 0^{1 \, x \, m_6} \\ 0^{1 \, x \, m_1} & 0^{1 \, x \, m_2} & 0^{1 \, x \, m_3} & 0^{1 \, x \, m_4} & 0^{1 \, x \, m_5} & C_{\mathrm{Exctn_6}}{}^{1 \, x \, m_6} \end{bmatrix} \tag{12}$$

where the dimension of the various submatrices is indicated with superscripts, and $\mathrm{m_i}$ is the dimension of the state-space system for the i_{th} DOF of platform motion. $0^{\mathrm{m_i \; x \; m_j}}$ is the zero matrix with dimensions $\mathrm{m_i \; x \; m_j}$.

The state-space models are valid for a fixed wave direction heading (between -180 and +180 degrees (deg.)). The wave direction convention follows the convention used in HydroDyn, as described in [2], Section 4.3.2 on waves. We will describe this input in more detail in Appendix A.

We now compare the calculated wave forces between the original IFT method and the wave forces calculated from the state-space model approximation for two particular floating platforms.

5. Wave force calculation comparisons

We want to compare the state-space model method of calculating wave forces on the platform with the standard method involving the IFT calculations in HydroDyn. We want to assess the approximate order of the state-space models (number of states) needed for accurate wave load calculations. We show these results for two different floating platforms: 1) the OC3 Hywind spar platform [12], and 2) the OC4 semi platform [13]. Table 1 shows the properties of these two platforms.

Table 1: FOWT platform model dimensions

		OC3-Hywind spar	OC4-Semi
Mass including ballast	[tons]	7466	13473
Volume of displaced water	$[m^3]$	0.803×10^4	1.39×10^4
Draft	[m]	120.0	20
Breadth	[m]	9.4	74

For both platform models, the panel code Wamit [9] was used with a constant frequency resolution to generate data needed to determine the platform FRFs. The non-causal IRFs were then calculated by the MatLab scripts and then time-shifted to arrive at causal IRFs. This time delay was set at $t_c = 10$ sec. for both platforms. Figure 5 shows the non-causal and time-shifted causal IRFs for the OC3 spar platform for the surge and pitching DOFs. Results for the OC4 Semi platform are similar and are not shown. The wave heading direction was set at zero degrees for both cases.

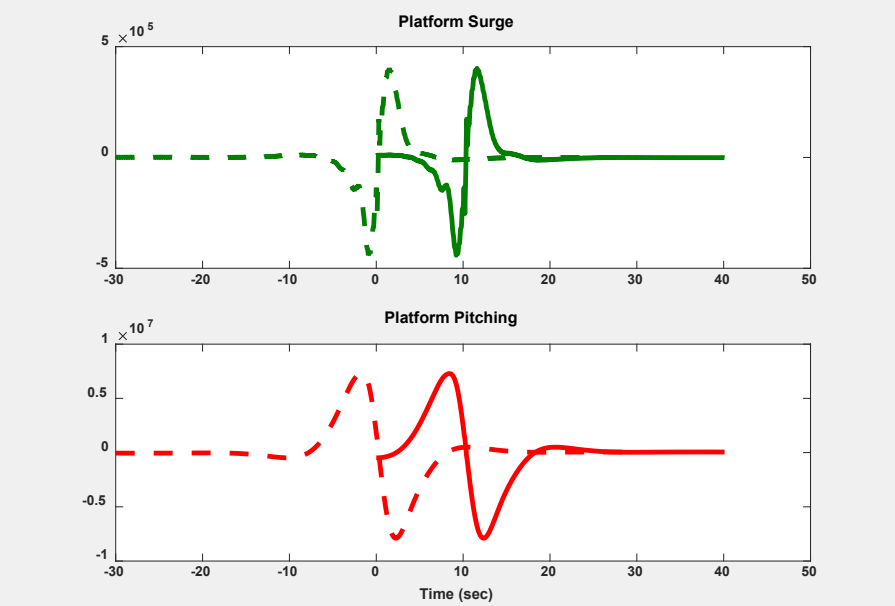

Figure 5. Non-causal and causal platform surge and pitching impulse response functions for the OC3 Spar platform.

We compare impulse responses and wave force time histories between the various models. Figure 6 shows the IRF comparisons for the OC3 Spar. The blue curve ($K_{\mathrm{Exctn_c}}$) represents the causal IRF to be approximated. The red curve (high order ss approx) is the impulse response from the highest-order fitted state-space model (approximately 400 states) obtained with Matlab's **imp2ss** function. The other curves represent the impulse responses from the reduced order state-space models with 4-, 6- and 8-states per load component. These models have been calculated from the high order state-space model by invoking Matlab's **balmr** command.

The impulse response from the highest order state-space model (red curve) produces an accurate representation of the causal IRF (in fact it hides the original IRF). Some noise is evident in this response, especially for time near 0 sec. This noise could be a result of the time-step (0.1 sec.) used in the IRF data. Impulse responses from the reduced order state-space models replicate the original causal IRF with increasing accuracy as the number of states is increased, with the 8-state model providing the best approximation. Use of even higher order state-space models could improve the replication of the causal IRFs.

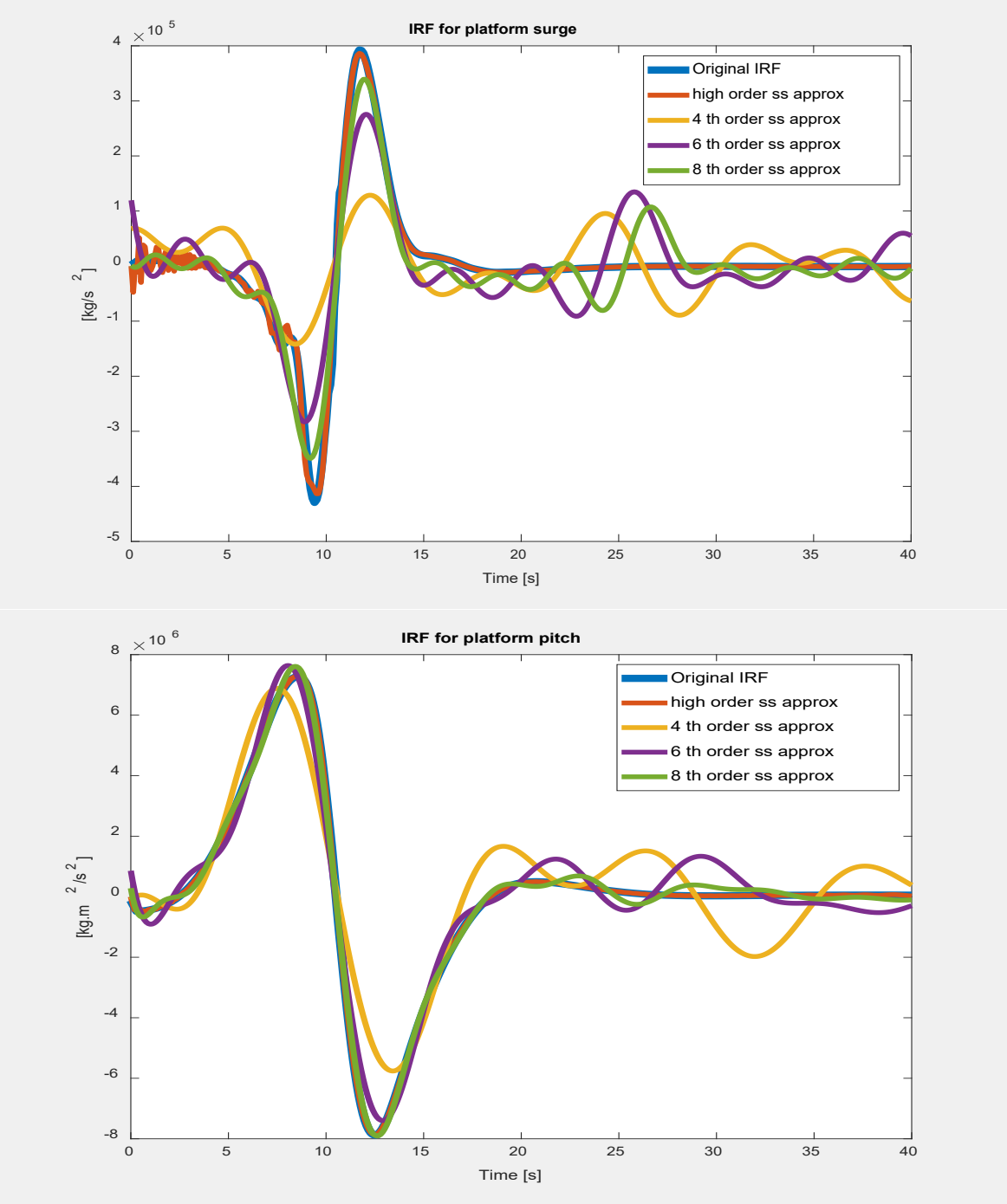

Figure 9. IRF Approximations for platform surge and pitching degrees of freedom for the OC3 spar platform.

Examination of the calculated wave forces provides even more insight into the required order of the state-space models necessary for accurate wave force calculations. We first compare calculated wave forces for the OC3 spar platform for a regular wave case. The regular wave had a period of 12.5 sec. and a height of 5 m.

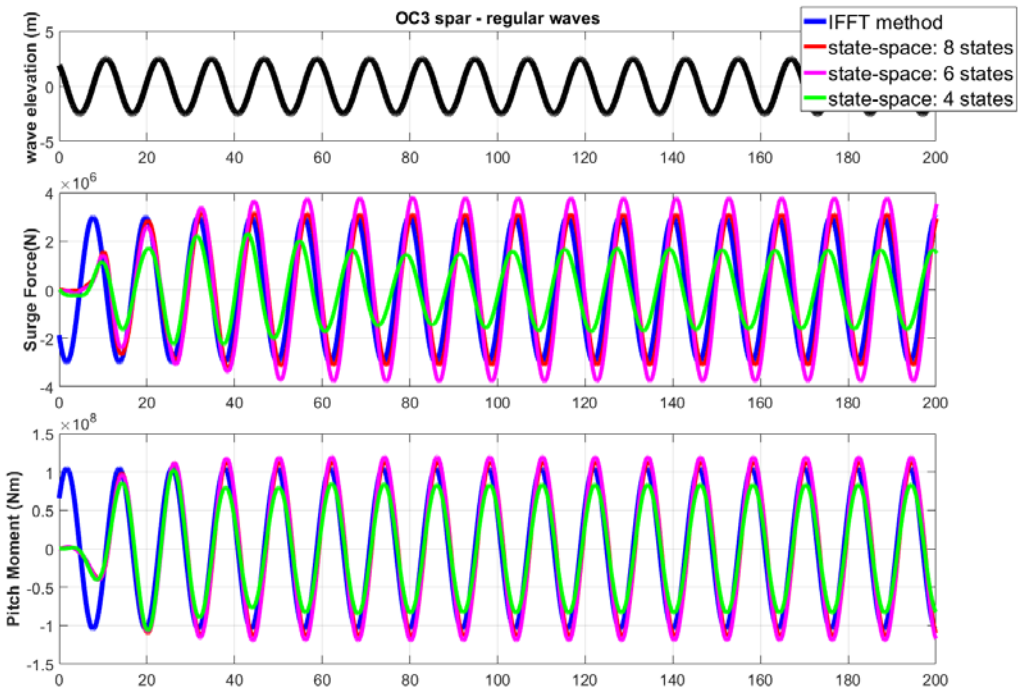

Figure 7. Comparison of wave forces calculated by the FFT and state-space model for the OC3 spar regular wave case.

Figure 7 shows comparisons between the IFT wave force calculations and results from the order 4-, 6- and 8-state models for the OC3 platform surge force and pitching moment for the regular wave case. In general, the results from the state-space models better replicate the IFT results as the number of states increases, with the best results from the 8-state model. The 4-state model does a poor job of replicating the IFT results. The 6-state model tends to overpredict the peaks and underpredict the troughs of the wave surge force and pitching moment.

Next, we perform this comparison for an irregular wave case for the same platform. This case has the same dominant wave frequency and height (12.5 sec. period, height 5m.) as the regular wave case. Figure 8 shows the comparisons for the OC3 spar platform's surge force and pitching moment. The trends in these results are very similar as for the regular wave case, with the 8-state model replicating the IFT calculation with the most accuracy. Again, the 4-state model produces the poorest replication and the 6-state model tends to overpredict the peaks and underpredict the troughs in the wave surge force and platform pitching moment.

In all of these results, the state-space model results show a start-up transient (which results

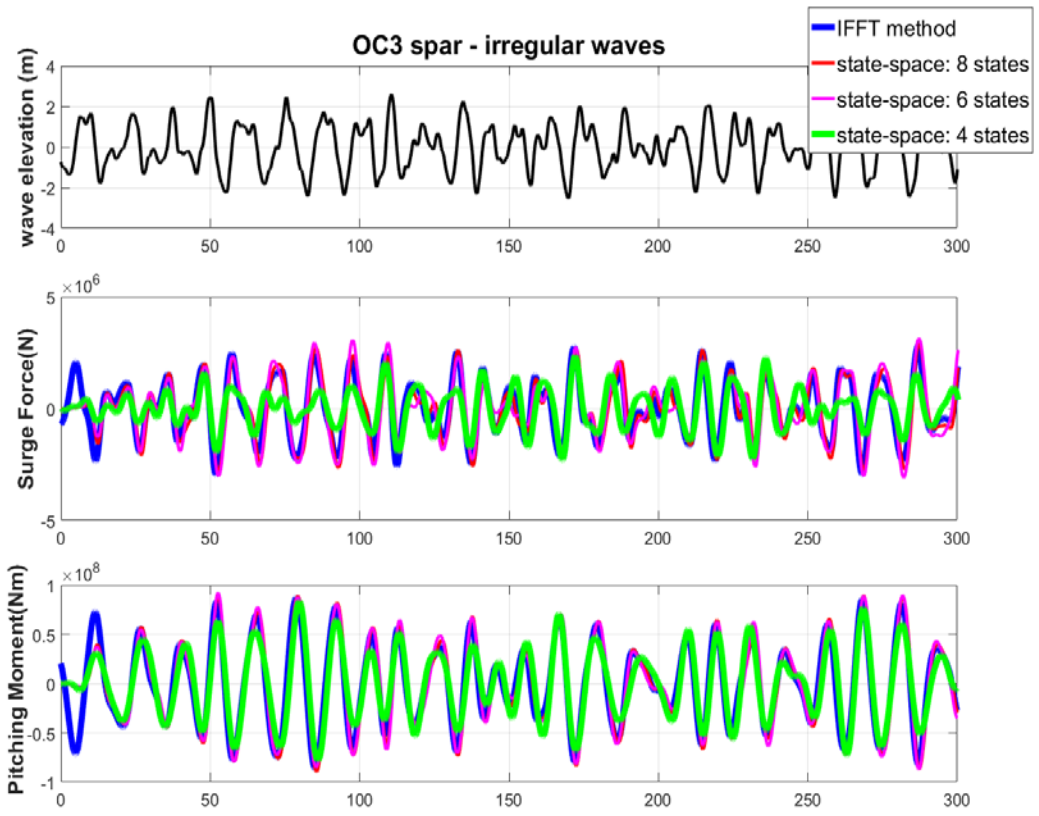

Figure 8. Comparison of wave forces calculated by the FFT and state-space model for the OC3 spar irregular wave case.

from initializing the states to zero at time zero) that decays in approximately 20 seconds after which the persistent response due to wave inputs is dominant.

These same comparisons are made for the OC4 semi platform. First, we compare IRFs in Figure 9 for the OC4 Semi. Again, the blue curve ($K_{\mathrm{Exctn_c}}$) represents the causal IRF to be

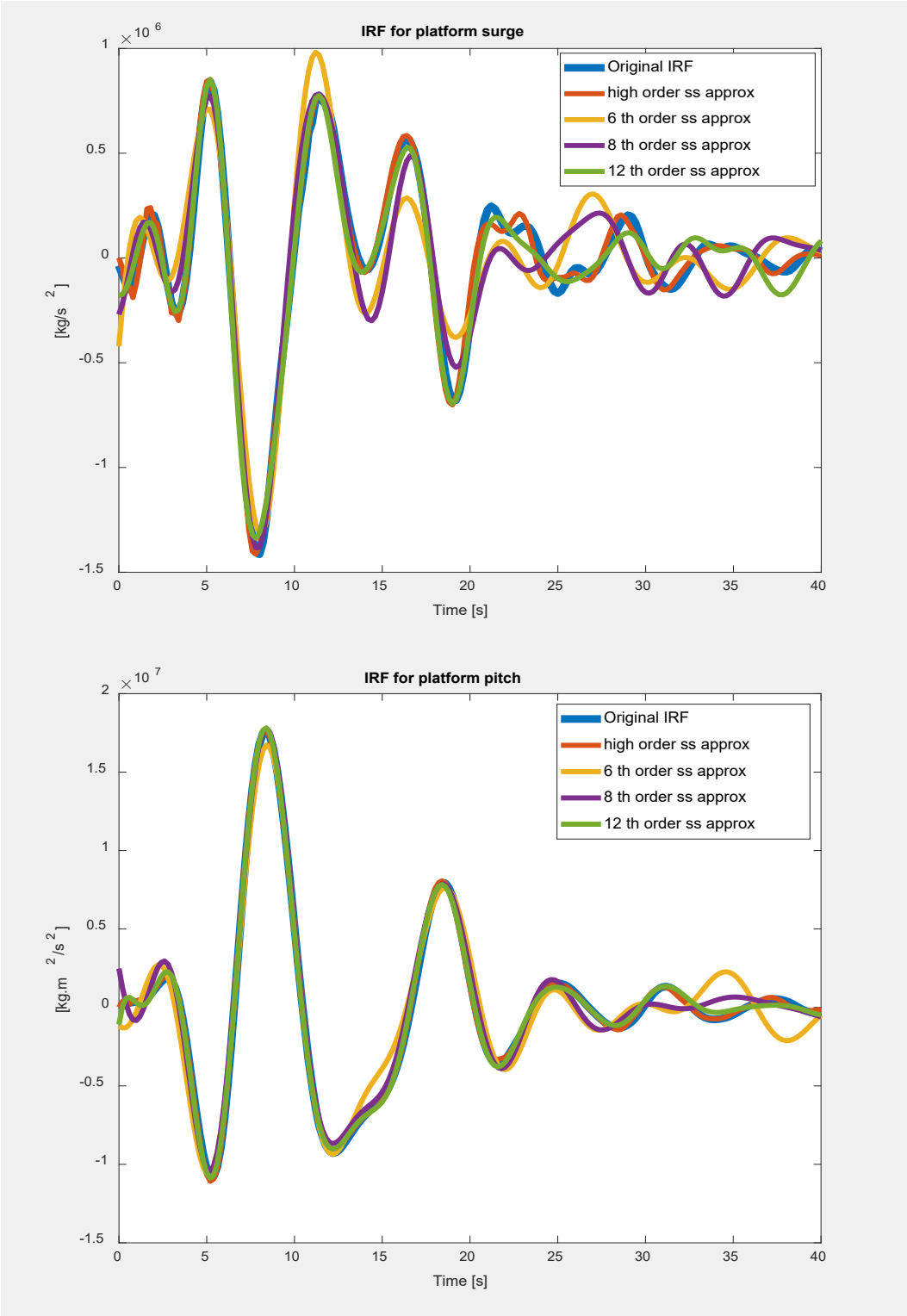

Figure 9. IRF Approximations for platform surge and pitching degrees of freedom for the OC4 semi platform.

approximated. The red curve (high order ss approx) is the impulse response from the highest-

order fitted state-space model (at least 200 states). The other curves represent the impulse responses from the reduced order state-space models with 6-, 8- and 12-states per load component. In general, we found that the OC4 semi platform required more states in the state-space model for accurate IRF approximations than the OC3 spar. Figure 9 shows that the 12-state model does the best job of approximating the original IRF. The lower order state space models give less accurate approximations.

Next, we compare calculated wave forces between the different state-space models for the OC4 Semi platform. The same wave height and dominant period (period 12.5 sec., height 5m.) are used for the OC4 semi case as for the OC3 Spar platform.

Figure 10 shows results from 6-, 8-, and 12-state models compared to the IFT method for the regular wave case. We see that all of the state-space models give good comparisons, with the 12-state model producing nearly identical results (except for a short start-up transient) to the IFT results. Use of the 6- state model give the least accurate replications of the IFT wave results. These results are very similar to the results for the OC3 Spar platform.

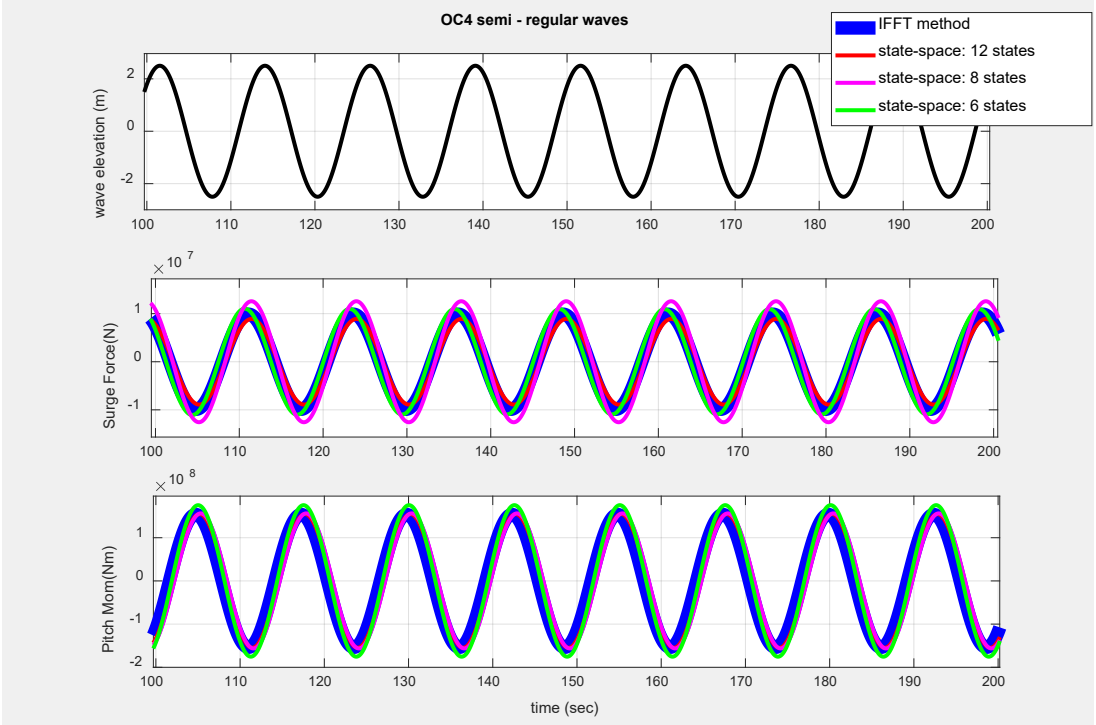

Figure 10. Comparison of wave forces calculated by the FFT and state-space model for the OC4 semi platform regular wave case.

Next, we perform this comparison for an irregular wave case for the same platform, with the same dominant wave period and height (12.5 sec. period, height 5m.). Figure 11 shows the comparisons for the OC4 spar platform's surge force and pitching moment. In general, the state-space models gave the best results for the platform pitching moment calculation. For the surge force calculation we found that the state-space models were not able to replicate the IFT results with as much accuracy as for the OC3 spar platform. The highest order state-space model (12 states) still had difficulty replicating the IFFT results. This could be due to the more complicated

structure of the OC4 semi platform. We calculated results using higher order state-space models (up to 20 states) but found that these models gave surge force calculations that were not much different than the 12-state model.

For this particular set of wave cases and these platforms, state-space models with approximately 8 states seemed sufficient for accurately calculating the platform pitch moment. For the OC4 semi platform, at least a 12-state model was needed to attempt to replicate the IFFT results, and even with this order state-space models, the IFFT results were replicated with only fair accuracy.

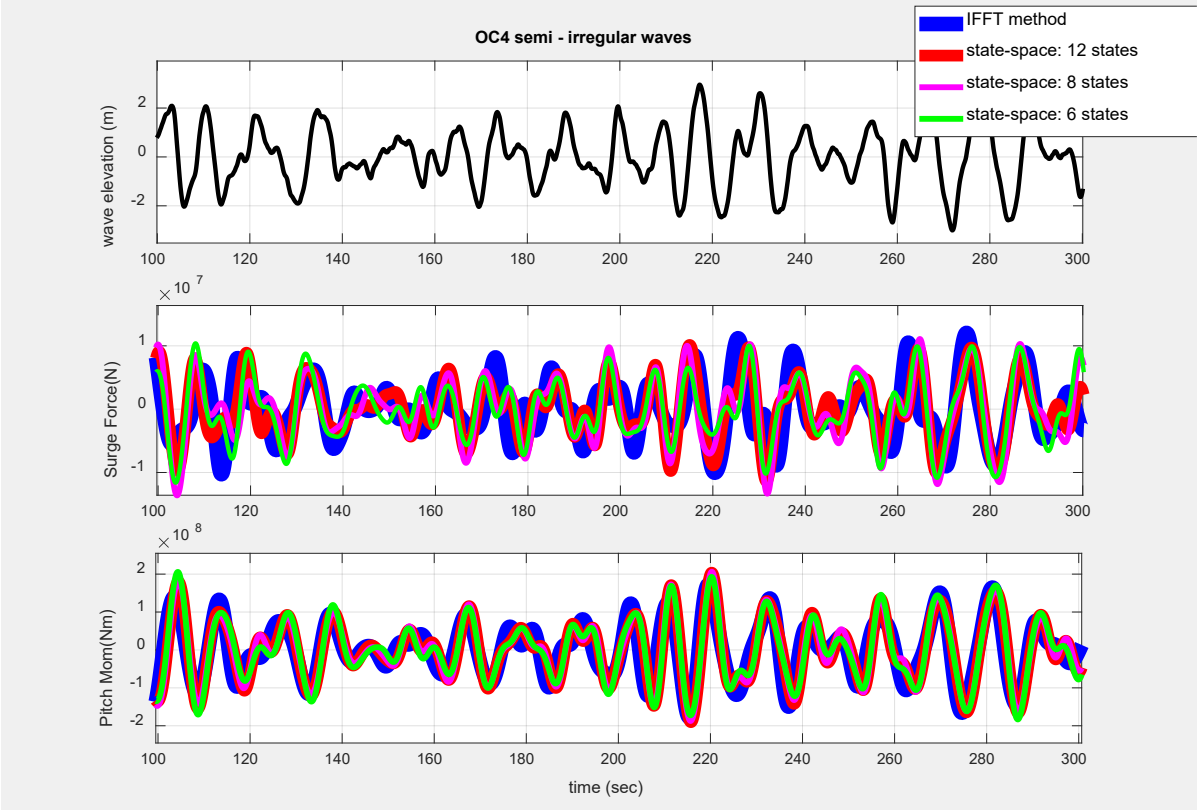

Figure 11. Comparison of wave forces calculated by the FFT and state-space model for the OC4 semi irregular wave case.

Next, we present a User's Guide to the MatLab routine that determine a state-space model for the wave excitation force system. This User's Guide is presented in Appendix A.

Appendix A: User's Guide

Steps in the Wave Excitation Force State-Space Modeling Process:

Let's describe the process of obtaining a state-space representation of the wave excitation forces acting on the platform. Figure A1 shows this process. This process has been programmed into a set of MatLab scripts contained in the scripts named **SS_Fitting_Wave_Excitation.m**, **CausalIRF.m,** and **Fit_StateSpace_Model.m**.

The first step is to read Wamit data and extract the platform's frequency response functions for the six platform DOFs. This process is performed in the overall script **SS_Fitting_Wave_Excitation.m**. The output of this script is the FRF $K_{\mathrm{Exctn}}(\omega)$, a 6x1 column vector containing an entry for each platform DOF.

Next, the Inverse Fourier Transform operation (using MatLab) is used to create the time-domain impulse response function (IRF), which in general is non-causal. A causal set of IRFs (again a 6x1 column vector) are calculated through time-shifting of the original IRFs. This process is performed in the script **CausalIRF.m**. This script inputs the FRF, performs inverse Fourier Transformations to produce $K_{\mathrm{Exctn}}(t)$, applies the user defined time delay t_c and outputs the causal IRF $K_{\mathrm{Exctn_c}}(t)$. This routine uses MatLab's built in Inverse Fourier Transform algorithm invoked through the **ifft** command [14]. The user will be prompted by the script to input a value for the time-delay t_c; this parameter is not contained in the input file for these scripts.

Next, a state-space model is fitted to the causal IRF in the script **Fit_StateSpace_Model.m**. First, the MatLab **imp2ss** command is used to obtain a high order (at least 200 state) state-space model from $K_{\mathrm{Exctn}}(t)$. Then Matlab's **balmr** command is invoked to obtain a reduced order state-space model approximation. The input to this routine is the causal IRF $K_{\mathrm{Exctn_c}}(t)$ and the outputs are the global state-space matrices described in equation [12] above.

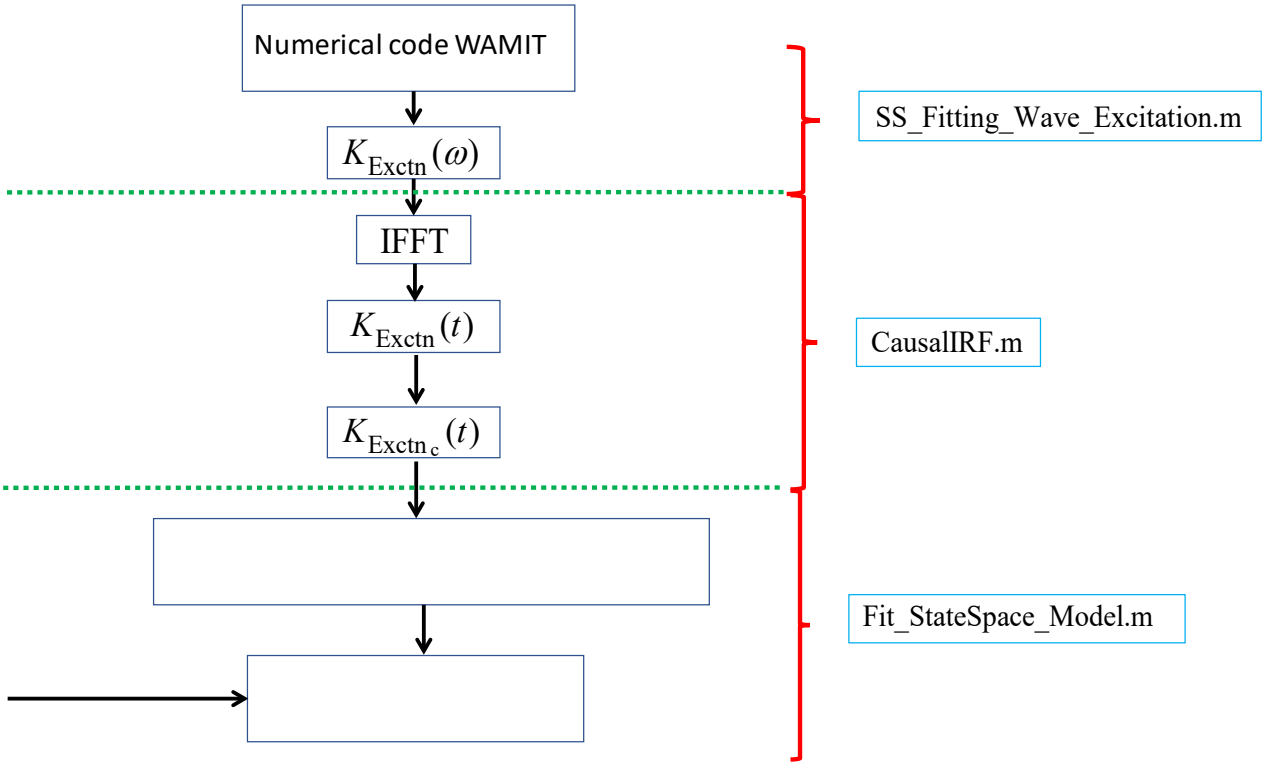

Figure A1. Steps in state-space model process and corresponding MatLab modules.

THE INPUT FILE

The input file, named "***Read_Wamit_Options.inp*** ", determines the program options, including the method used to compute the fitting. Please use the supplied example file as a reference. The file must contain the inputs shown in Table A.1.

The first line is the location of the Wamit files for the modeled platform. The second line indicates those DOFs being enabled for the state-space wave excitation model. The third line indicates the analysis time for the wave WaveTMax. This parameter sets the length of the incident wave kinematics time series and determines the frequency step used in the inverse FFT calculations ($\frac{2\pi}{WaveTMax}$). The fourth line inputs the time step for incident wave calculations (dT). This parameter also determines the maximum frequency in the inverse FFT ($\frac{\pi}{dT}$).

Table A.1: Input file Content

Option	Variable Name	Description
File location	Excite.FileName	Base name and location of the Wamit file for the desired platform. The location can be absolute or relative to the SS_Wave_Excitation_Fitting folder.
Degrees of Freedom Vector	Excite.DoF	[1x6] vector containing 1 or 0 if the corresponding DOF is enabled or not. It follows the order surge, sway, heave, roll, pitch and yaw. For 6 enabled DOF use [1 1 1 1 1 1].
Maximum wave time	Excite.WaveTMax	Analysis time for incident wave calculations (sec.).
Time step	Excite.dT	Time step for incident wave calculations (sec.).
Fit tolerance option	Excite.Fit	Fit required for the parametric model (max recommended 0.99).
Plotting option	Excite.ppmf	Plot the parametric model fit (0 or 1)
Method of order reduction	Excite.fmt	Manual (1) or Automatic (0) state-space model order reduction
Maximum number of iterations	Excite.maxiter	Maximum number of fitting iterations for the Automatic model order reduction method
Water density value	Excite.WtrDen	Water density (kg/m^3)
Gravity	Excite.Grav	Gravitational acceleration (m/s^2)
Wave direction	Excite.WaveDir	Incident wave propagation heading direction (deg.)
Output file name	Excite.OutFileName	File name descriptor

The fifth line determines the target value for the tolerance R_{target} in equation [10]. This parameter is used only if the Automatic model order reduction method is chosen (to be described next). The value of R is calculated via equation [10] for each iteration in the model reduction loop. The model reduction process is concluded when the value of R reaches or exceeds R_{target}. The sixth line allows the user to choose the maximum number of iterations in the automatic order reduction process. There may be situations in which it takes many iterations for the value of R to reach R_{target}. The user may want to place a limit on the number of iterations that can be performed, since a high number of iterations results in a very high order state-space model. This means that the value of R does not reach R_{target} but that the state-space model may meet other desired criteria.

The other lines in the input file represent various parameters, such as the value of water density, gravitational acceleration, and the dominant wave heading direction. The last line indicates the prefix name for the output files.

Please note that the user will be prompted to input the "causalizing" time delay t_c during script execution. This parameter is not included in the input file.

RUNNING SS_FITTING

Running SS_Wave_Excitation_Fitting requires a license for *MatLab* **and** the *Robust Control Toolbox*. Before running SS_Wave_Excitation_Fitting, make sure that SS_Wave_Excitation_Fitting *Source* is in the MatLab search path. The user should define all the inputs using the input file "***Read_Wamit_Options.inp***", as above.

We illustrate these steps for the OC3 Spar model described in Section 5. To begin running the script, the user simply types the command (on the Matlab command line):

[Newtime,ssExcite,Aglobal,Bglobal,Cglobal,Dglobal]=SS_Fitting_Wave_Excitation('Read_Wamit_Options.inp').

Upon invoking the command, the script will then launch the process and calculate the FRFs and resulting IRFs for each chosen platform DOF. The script first produces plots of the non-causal IRFs for each chosen platform DOF, as illustrated in Figure A2 (screen shot). These are the IRFs that have been calculated by invoking Matlab's **IFFT** routine on the FRF calculated from Wamit data.

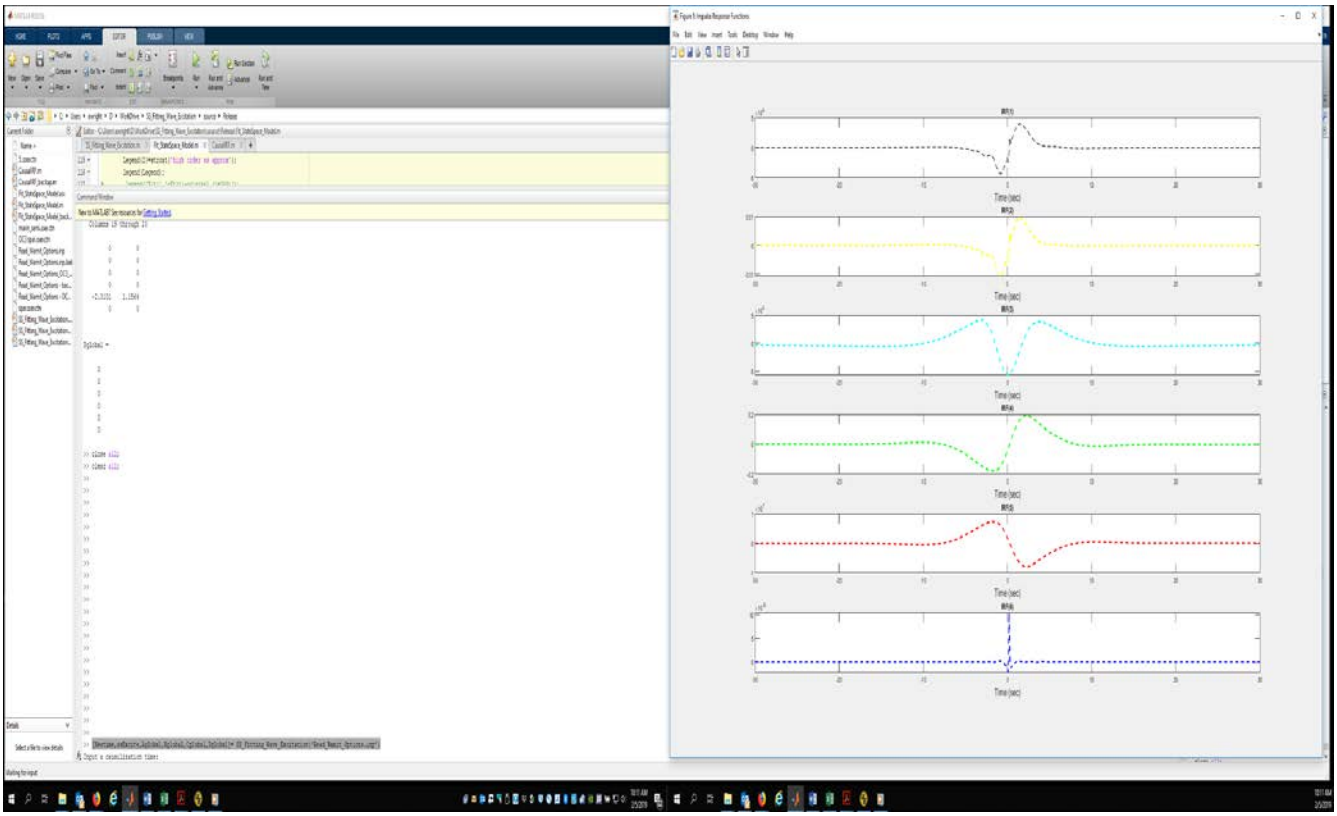

Figure A2: Screenshot after invoking the SS_Fitting_Wave Excitation Command.

Next, the user is prompted for the desired value of the time-delay t_c (sec.) for "causalizing" the IRFs (see Section 2.2). After the user inputs this value at the command line, the script will add the time-delayed "causal" IRFs to the plot, as illustrated in Figure A3 (here t_c = 10 sec.).

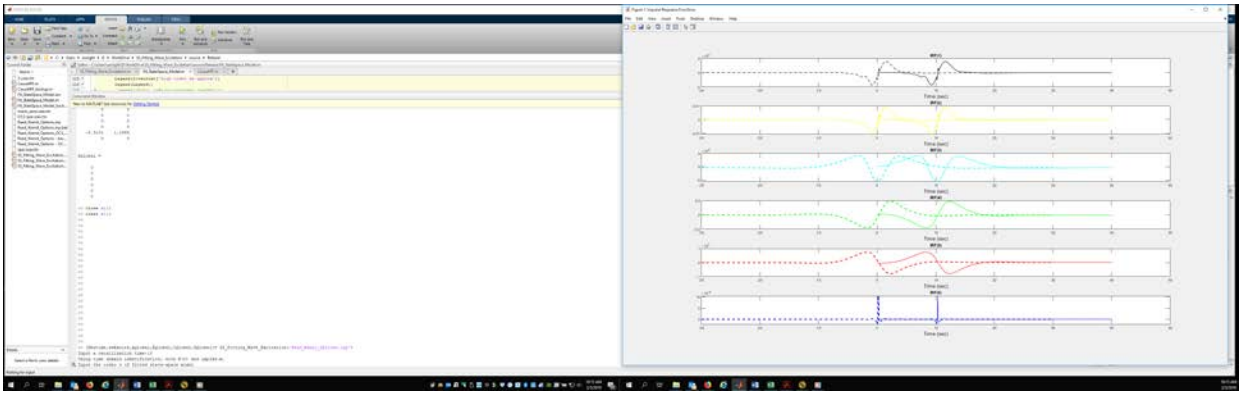

Figure A3: Screenshot after inputting value for the time-delay t_c.

The current script allows the user to input only one value for t_c; this value of t_c is used to "causalize" all of the resulting IRFs for all chosen platform DOFs. Future script refinements will allow the user to choose different values of t_c for different DOFs.

The script starts running through the model order reduction process. This is performed for each chosen platform DOF, in sequence. It first produces a plot showing the original IRF (produced by invoking the Matlab IFFT command on the FRF) and the IRF approximation based on the high-order state-space model (produced through invoking Matlab's **imp2ss** command). Figure A4 illustrates this plot.

The script then proceeds to calculate reduced order state-space models, by invoking Matlab's **balmr** command. The method of doing this is determined either by the manual method or automatic method of model order reduction (see last section)

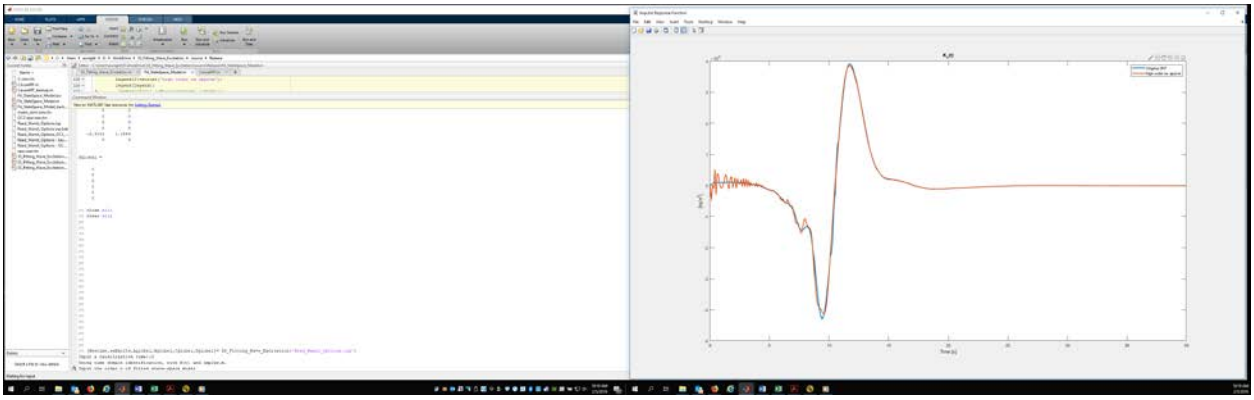

Figure A4: Screenshot after inputting value for the time-delay t_c.

If the manual order reduction method is chosen, the script prompts the user for the model order "n." The script then calculates a reduced order state-space model based on this value of n. The IRF resulting from this reduced order model is added to the IRF plot. Figure A5 shows a screen shot when n=4.

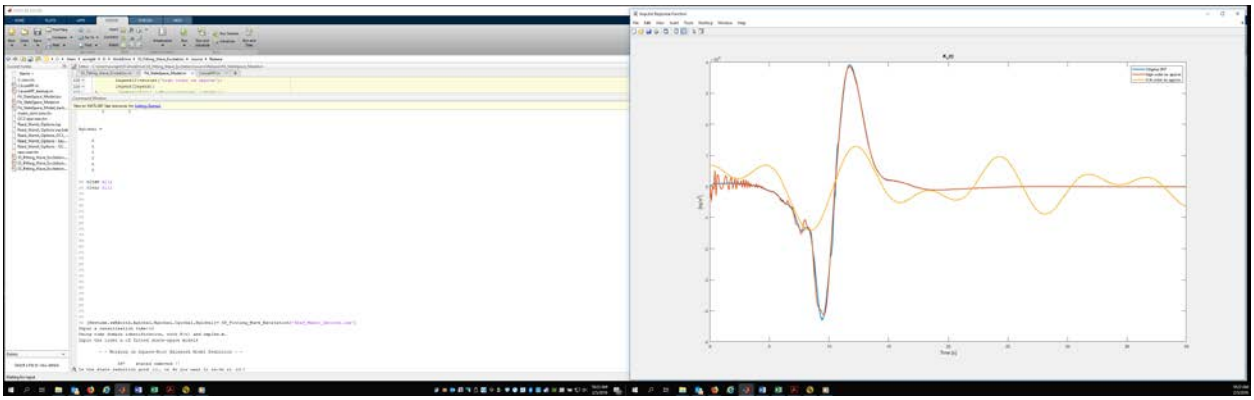

Figure A4: Screenshot after inputting the first value of the order of the reduced order model (n=4 in this example).

The user can then obtain improved models by increasing the model order n. In the manual method, this is based on the experience of the user and an "eyeball" evaluation of the IRF approximations to the original IRF. The script will ask the user if the current approximation is adequate or if a new fitting should be performed. An input of "0" by the user signals the script to repeat the process with a new value of n, as input by the user. An input of "1" at the command line signals the script to stop with the last reduced order model. The script proceeds to move on to the next chosen platform DOF.

If the automatic model order reduction method is chosen, the user is not prompted for the value of n. The value of n is increased by one iteratively (starting with a value of n=2) until the R criteria (see equation [10]) is reached. This is based on the R_{target} value set in the input file (see above) along with the value of the maximum number of iterations allowed in this process (maxiter) . The script will continue increasing n until the R criteria is met, or the maximum number of iterations (maxiter) is reached, whichever occurs first. The final reduced order state-space model is based on the value of n when the criteria is met. The script calculates and displays the IRF approximation from the final reduced order state-space model. This procedure removes some of the "guess work" involved when using the manual method of order reduction.

While running the script using the automatic order reduction method, the value of R^2 as well as the iteration number will be displayed on the command line. If the maximum number of allowed iterations has been reached before the R criteria has been met, a message will be displayed on the command line to that effect. The script runs through all user selected platform DOFs and produces plots for the IRF approximations, as shown in the screenshot of Figure A.5.

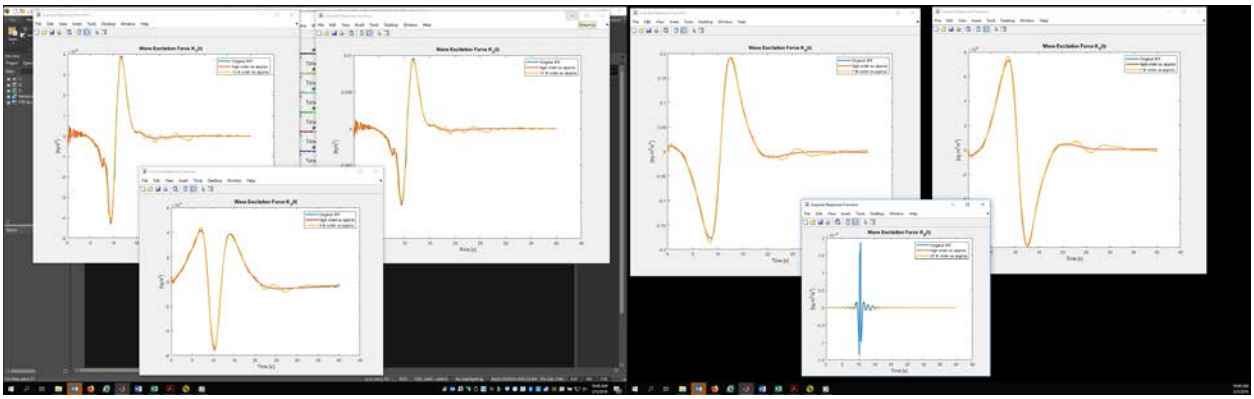

Figure A5: Screenshot at the conclusion of using the automatic order reduction method.

Regardless of the reduction method chosen (user selected or automatic) the script finally produces the global the state-space matrices $\mathrm{A}_{\mathrm{global}}$, $\mathrm{B}_{\mathrm{global}}$, and $\mathrm{C}_{\mathrm{global}}$ (which correspond to A_{Exctn}, B_{Exctn}, and C_{Exctn} in equation [12]) and makes these matrices available in the Matlab workspace. It also produces an output file containing the global state-space matrices as described below.

THE OUTPUT FILE

The output file containing the global state-space matrices is formatted to be read by OpenFAST's HydroDyn module [2]. It contains miscellaneous parameters and the global state-space matrices. The output file has the prefix indicated by the value of the input parameter "Excite.OutFileName" (see Table A.1 above). The file extension is named "ssexctn." The contents of this file are illustrated in Table A.2, which shows a screenshot example.

Table A.2: Output file content

Description	Variable Name
Header descriptor line	
Wave Heading Angle (deg.)	Excite.WaveDir
Time delay for causal IRF (t_c) (sec.)	Time delay used in causalization
Order of global state-space model (total number of states)	ExcitationStates
Order of the individual state-space matrices corresponding to each DOF	ExcitationStatesperDOF
Global A-matrix (A_{Exctn})	Aglobal
Global B-matrix (B_{Exctn})	Bglobal
Global C-matrix (C_{Exctn}) (Note: D_{Exctn} is assumed to be the zero matrix)	Cglobal

Retrieving Files from the Archive:

TBD ……..

You can download the SS_Wave_Excitation_Fitting archive from the web page *http://wind.nrel.gov/designcodes/postprocessors/.....T*BD.... Create an appropriate folder somewhere on your file system and put this file there. When you double click on the archive from Windows Explorer, it will create some files and folders. To use the scripts, you need to add SS_Wave_Excitation_Fitting's *Source*, folder to the MatLab search path.

TBD ……..

Distributed Files:

TBD ……..

SS_Wave_Excitation_Fitting includes the following files:

Change_log.txt -Log file with the updates of the current version
Disclaimer.txt -Disclaimer file

SS_Wave_Excitation_Fitting_Manual.pdf -Theory and User Manual (this document)

Read_Wamit_Options.inp	-Sample input file with user defined options
Source/SS_Wave_Excitation_Fitting.m	-Main MatLab File
Source/CausalIRF.m	-MatLab routine responsible to calculate a causal impulse response function from the Wamit data.
Source/Fit_State_Space_Model.m	-MatLab routine responsible to fit the state-space model to the causal impulse response function
Verification/OC3spar/	-Folder containing the results files using the OC3Hywind spar buoy as reference platform
Verification/OC4 Semi/	-Folder containing the results files using the OC4 Semi as reference platform

TBD ……..

Acknowledgments

The MatLab routines were developed by Alan Wright, based on the work of Tiago Duarte, who developed similar routines for the wave radiation force system. Jason Jonkman, Amy Robertson, and Greg Hayman provided valuable contributions and integration of this method into OpenFAST's HydroDyn module.

Appendix B: Proof of Equation (7)

$$F^{\text{waves}}(t) = \int_{-\infty}^{\infty} K_{\text{Exctn}}(t-\tau)\varsigma(\tau)d\tau = K_{\text{Exctn}}(t) * \varsigma(t)$$

But

$$K_{\text{Exctn}_c}(t) = K_{\text{Exctn}}(t - t_c)$$

So

$$F^{\text{Waves}}(t) = \int_{-\infty}^{\infty} K_{\text{Exctn}_c}(t + t_c - \tau)\varsigma(\tau)d\tau$$

Let: $\overline{\tau} = \tau + t_c$

$d\overline{\tau} = d\tau$

$$F^{\text{Waves}}(t) = \int_{-\infty}^{\infty} K_{\text{Exctn}_c}(t + t_c - \overline{\tau} - t_c)\varsigma(\overline{\tau} + t_c)d\overline{\tau}$$

$$= \int_{-\infty}^{\infty} K_{\text{Exctn}_c}(t - \overline{\tau})\varsigma(\overline{\tau} + t_c)d\overline{\tau}$$

$$= K_{\text{Exctn}_c}(t) * \varsigma(t + t_c)$$

So

$$F^{\text{Waves}}(t) = K_{\text{Exctn}_c}(t) * \varsigma(t + t_c) = K_{\text{Exctn}}(t) * \varsigma(t)\,.$$

References

1. Web page https://nwtc.nrel.gov/OpenFAST (accessed May 7, 2018).
2. Jonkman, J. M., Robertson, G. J., and Hayman, G. J. "HydroDyn User's Guide and Theory Manual." Web page https://wind.nrel.gov/nwtc/docs/HydroDyn_Manual.pdf. Draft report.
3. Jonkman, J. M. *Dynamics Modeling and Loads Analysis of an Offshore Floating Wind Turbine*. Ph.D. Thesis. Department of Aerospace Engineering Sciences, University of Colorado, Boulder, CO, 2007; NREL/TP-500-41958. Golden, CO: National Renewable Energy Laboratory.
4. Jonkman J., Wright, A., Hayman, G., and Robertson, A. "Full-system Linearization for Floating Offshore Wind Turbines in OpenFAST." ASME 2018 1st International Offshore Wind Technical Conference (American Society of Mechanical Engineers), pp. V001T01A028-V001T01A028. 2018.
5. Duarte, T.; Alves, M.; Jonkman, J.; and Sarmento, A. "State-Space Realization of the Wave-Radiation Force within FAST." *32nd International Conference on Ocean, Offshore, and Arctic Engineering (OMAE2013), 9–14 June 2013, Nantes, France* [DVD-ROM]. OMAE2013-10375. Houston, TX: The American Society of Mechanical Engineers (ASME International) Ocean, Offshore and Arctic Engineering (OOAE) Division, June 2013; ISBN 978-0-7918-5542-3; NREL/CP-5000-58099. Golden, CO: National Renewable Energy Laboratory.Ogata, K., 1990, *Modern Control Engineering*, Prentice-Hall, Inc., Englewood Cliffs, NJ.
6. Wep page https://nwtc.nrel.gov/SS_Fitting (accessed May 7, 2018).
7. Yu, Z. and Falnes, J. "State-space Modeling of a Vertical Cylinder in Heave." *Applied Ocean Research*, Vol. 17, Issue 5, pp. 265-275, 1995.
8. Lemmer, F., Raach, S., Schlipf, D., and Cheng, P. "Parametric Wave Excitation Model for Floating Wind Turbines." *13th Deep Sea Offshore Wind R&D Conference, EERA DeepWind'2016*, January 20-22, 2016. Trondheim, Norway. Energy Procedia 94 (2016) 290-305.
9. Wamit User's Manual Version 7.0. Technical Report: MIT, 2011. URL: http://www.wamit.com/manualupdate/V71_manual.pdf.
10. Web page: https://www.mathworks.com/help/releases/R2018b/pdf_doc/robust/
11. Laub, A. J., Heath, M. T., Page, C. C., and Ward, R. C. "Computation of Balancing Transformations and other Applications of Simultaneous Diagonalization Algorithms." IEEE Trans. On Automatic Control., AC-32, pp. 115-122, 1987.
12. Jonkman, J. "Definition of the Floating System for Phase IV of OC3." NREL/TP-47535. May 2010.
13. Robertson, A. N., and Jonkman, J. M. "Loads Analysis of Several Offshore Floating Wind Turbine Concepts." Presented at the International Society of Offshore and Polar Engineers 2011 Conference. Maui, Hawaii. June 2011.